

# Analytical descriptions of high-Tc cuprates by introducing rotating holes and a new model to handle many-body interactions

Shinichi Ishiguri

Nihon University

1-2-1 Izumi-Cho, Narashinoshi, Chiba 275-8575 JAPAN

TEL: +81-47-474-9143

Email: [ishiguri.shinichi@nihon-u.ac.jp](mailto:ishiguri.shinichi@nihon-u.ac.jp)

## Abstract

This paper describes all the properties of high-Tc cuprates by introducing rotating holes which are created by angular momentum conservations on a two dimensional CuO<sub>2</sub> surface, and which have a different mass from that of a normal hole due to the magnetic field energy induced by the rotation. This new particle called a macroscopic boson describes doping dependences of pseudo gap temperature and the transition temperature at which an anomaly metal phase appears. In addition, it also describes all the properties of the anomaly metal phase, using findings from our previous article [1]. Furthermore, the present paper introduces a new model to handle many-body interactions, which results in a new statistic equation. A partition function of macroscopic bosons describes all the properties of the anomaly metal phase, which sufficiently agrees with experiments. Moreover, the above-mentioned statistic equation describing many-body interactions accurately explains why high-Tc cuprates have significantly high critical temperatures, which indicates that the source of the characteristic stems from pseudo gap energy. By introducing a macroscopic boson and the new statistic model for many-body interactions, the present paper uncovered the mystery of high-Tc cuprates, which have been a challenge for many researchers. Moreover, in the present paper, pure analytical calculations are conducted. These calculations agree with experimental data which do not employ numerical calculations or fitting methods but employ many actual physical constants.

## Keywords:

High-Tc cuprates, macroscopic boson, many-body interactions, pseudo gap, critical temperature, anomaly metal phase, conservation of angular momentum, attractive force, Cooper pair

## 1. Introduction

### 1.1 Brief summary of the paper

In particular, this paper theoretically describes properties of high-Tc cuprates. That is, we clarify why high-Tc cuprates has considerably high temperature as the transition.

Based on results from our previous paper [1], the present paper describes pseudo gap temperature  $T^*$  and transition temperature  $T_0$  at which the anomaly metal phase appears, as well as critical

temperatures  $T_c$ . Moreover, the anomaly mental phase such as Hall coefficient  $R_H$ , electron specific heat coefficient, etc., are described from the findings above.

Furthermore, we have established a new model for many-body interactions and thus, using this model, the mechanism of high- $T_c$  cuprates, with considerably high temperature  $T_c$ , is uncovered.

### 1.2 *Background*

The significance of the present paper will be better understood with a review of the fundamental concept of superconductivity. Although several significant advancements have been presented, from the initial discovery of a superconductor,, the most impressive discoveries are the  $\text{CuO}_2$ -based superconductors (i.e., high- $T_c$  cuprates) [2]. This is because, prior to this finding, superconductors generally require significantly high refrigeration because of their lower critical temperature (about 20 K). However, because they have higher  $T_c$  than  $\text{LN}_2$ , high- $T_c$  cuprates received the widest attention and interests from condensed matter physics researchers, as well as researchers in technologies who showed interest in the technical merits when applied to superconducting magnetic energy storage, energy transmitting [3-5], and so on. Thus, initial findings showed that high- $T_c$  cuprates involved many condensed matter physics and technologies researchers.

However, condensed matter physics researchers investigated high- $T_c$  cuprates for deeper reasons. That is, they are the first case at which the standard band model and the Bardeen-Cooper-Schrieffer (BCS) theory are not applied, which implies that novel physical phenomena occurred. (Recent H-based superconductors [6] with extremely high pressures have high potential to be applied to the BCS theory.) Nevertheless, many claimed that it is related to many-body interactions, which made many theoretical researchers' approach to the mechanism difficult. It is obvious that, as an analogy to the BCS theory, the use of quantum field theory is not adequate because quantum field theory is too abstract and does not reflect the fact that a phenomenon in condensed matter physics involves many actual physical constants. Although many articles about the experiments have been reported [7-13], no theory describes all the experimental data. There are several reasons for this: many-body problems are essential and there is no information about the kind of force that combines a Cooper pair in high- $T_c$  cuprates.

Consequently, existing theories have attempted to describe the mechanism of high- $T_c$  cuprates using either Fermi-liquid model or resonating valence bond (RVB) model [14-17]. However, these theories have undetermined parameters, which inevitably leads to numerical or fitting methods. We must mention that they are insufficient, because many related and actual physical parameters are involved when the properties of high- $T_c$  cuprates are considered. For example, several researchers claim that, because of magnetic field interactions, the nature of force to combine a Cooper pair must

be spin interactions. However, as mentioned later in this paper and previous our paper [1], magnetic field interactions are not generally only spin interactions. Furthermore, if the interaction was defined as the spin interaction, they could not explain why other many physical parameters such as phonons are related.

Although many theories that discuss the nature of force to combine a Cooper pair and the source of pseudo gap using RVB model or Hubbard model exist, few theoretical articles address the anomaly metal phase and the transition temperature  $T_0$  at which the anomaly metal phase appears.

In particular, a number of themes and problems to theoretically solve the mechanism of high- $T_c$  cuprates exist despite the number of experiments conducted and thus, researchers continue to investigate other possibilities of high- $T_c$  cuprates.

Recent discussions showed that because there is no future solution to high- $T_c$  cuprates, most researchers now take their themes to topology insulators in order to publish more articles within a short term. That is, for young students to become researchers, because of the complexities of high- $T_c$  cuprates. young researchers are not interested in researching high- $T_c$  curprates and instead other materials are focused on. This is because the busy schedules of researchers do not allow the needed ample study time.

In the present paper, however, we believe that studies on high- $T_c$  cuprates are not irrelevant. Rather, we would like to emphasize again the importance of this basic study.

### 1.3 *Outline of the theory in this paper*

The present paper describes further facts based on the previous our paper [1]. In our previous paper, critical temperatures  $T_c$  on doping were described, which agrees with experiments. The present paper describes basically the anomaly metal phase properties and why high- $T_c$  cuprates exhibit significantly high critical temperature when many-body interactions are considered.

What describes properties such as the anomaly metal phase is not a net hole-carrier but a rotating hole. This rotation occurs because, under a transition temperature  $T_0$ , holes experience complete 2D  $\text{CuO}_2$  surface, i.e., 2D motions are generally allowed by angular momentum conservations. This rotating hole (referred to as a macroscopic boson) differs from a normal net hole, because this macroscopic boson has self-induced magnetic field energy. Thus the mass of a macroscopic boson is much larger than that of a single hole. Moreover, the radius of a macroscopic boson is approximately in order of a  $\text{CuO}_2$  cell (i.e., about 1 nm).

Basically, the mass of macroscopic bosons provides pseudo gap temperature  $T^*$ . These macroscopic bosons behave according to an approximated partition function in terms of bosons.

Furthermore, a particular form of this partition function describes the anomaly metal phase properties.

Subsequently, we established a model to handle many-body interactions, which describes why high-T<sub>c</sub> cuprates exhibit significantly high critical temperature. In addition to Coulomb interaction, magnetic field interaction between macroscopic bosons are included in our model. It predicts extremely short coherence (i.e., about 1 nm) up to about 140 K (i.e., a critical temperature), but at further temperatures the relative distance suddenly becomes  $10^{-7}$  m order. As mentioned in our previous paper [1], a method to combine a Cooper pair is Lorentz force which only appears when two charged particles move at the same velocity due to the law of action and reaction. Therefore, when the relative kinetic energy of two macroscopic bosons becomes zero, the above-mentioned model predicts that the relative distance between the two macroscopic bosons becomes zero, with the net coherence of two holes in order of CuO<sub>2</sub> cell, i.e., 1 nm. Our model explains why high-T<sub>c</sub> cuprates have significantly high critical temperature because the magnitude of the magnetic field interaction by macroscopic bosons is large.

#### *1.4 Brief review of our previous paper*

As described in details in the review section of the present paper, we briefly explain a method of force to combine a Cooper pair.

As mentioned, when two charged particles have the same velocities, i.e., the relative kinetic energy is zero, these two particles experience an attractive force with each other, which stems from the Lorentz force. This phenomenon can be understood using an analogy that two macroscopic parallel current leads experience an attractive force with each other according to electromagnetism. Next, we consider that these current leads are shortened to a wavelength of a microscopic quantum particle. Even at this situation, as long as the wave numbers of two particles are equal, it is assumed that two moving charged particles still experience the attractive force with each other. As will be mentioned in the review section of the present paper, this is a source of attractive force to combine a Cooper pair, which results in a critical temperature T<sub>c</sub>.

#### *1.5 Summary of significances in this paper*

As discussed in the Discussion section, consider the summary of significances in the present paper.

- 1) It has uncovered the source of mysteries in high-T<sub>c</sub> cuprates, i.e., the presence of a macroscopic boson.
- 2) It has succeeded in describing the anomaly metal phase with pure theory, which has no fitting or numerical calculations and which agrees with experiments.

- 3) It has established a new model to handle general many-body interactions, and using this model, this paper has clarified why high-T<sub>c</sub> cuprates have so high critical temperature.

#### 1.6 *Entire contents of the paper*

The entire paper is organized as follows:

In the theory section, we describe the followings:

- 1) A macroscopic boson and the partition function the bosons obey are presented.
- 2) Pseudo gap energy and the temperature T\* are calculated.
- 3) A transition temperature T<sub>0</sub> at which the anomaly metal phase appears is described.
- 4) Using the partition function, Hall coefficient equation RH dependent on both temperatures and doping is derived. Moreover, electron specific heat coefficient dependent on doping is also obtained.
- 5) A new model to handle many-body interactions is established.

In the result section:

- 1) Theoretical T<sub>c</sub>, T\*, and T<sub>0</sub> dependences on doping are shown.
- 2) The dependence of the Hall coefficient RH and electron specific heat coefficient on doping are presented.
- 3) As a result of establishing new model to handle many-body interactions, relative distance between two macroscopic bosons per temperature is shown, which clarifies a point of critical temperature T<sub>c</sub>.

After the Discussion and Conclusion sections, an Appendix describes theoretically Curie temperatures in ferromagnetic materials such as Fe, using our above-mentioned model to handle many-body interactions.

## 2. Theory

### 2.1 *Introduction of new particle*

When considering a CuO<sub>2</sub> surface and when the refrigeration is sufficient that a hole wavelength becomes larger than that of the width of the surface, it is assumed that 2-dimension is completely formed. This implies that, on the surface, an angular momentum must be conserved. Thus, each hole takes a circle by self-rotating. At this time, because this rotating circle has magnetic field energy, we should consider that a new particle has been created. Going forward, we refer to this new particle as a

“macroscopic boson”. The schematic is shown in Fig. 1.

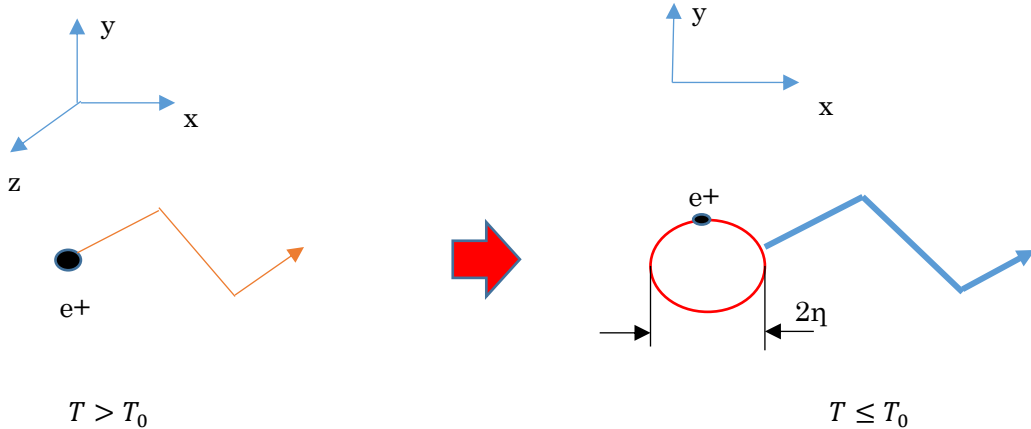


**Fig.1**

**Schematic of a macroscopic boson.** Normally, holes move in 3-dimension when their kinetic energy is high. However, when refrigeration reduces the momentum along z-direction, the complete x-y 2-dimensional motion is formed. Thus, a conservation of the angular momentum creates a rotation movement by a hole itself. Because a current circle by the rotation generates magnetic field energy, which determines the mass of this circle, this circle is essentially different from a normal hole. We will refer to this new particle as “a macroscopic boson.” Note that the radius  $\eta$  of a macroscopic boson is assumed to be in order of a CuO<sub>2</sub> cell (i.e. about 1 nm)

First, let us calculate the mass of a macroscopic boson. Using a magnetic flux, magnetic field energy is represented as

$$2U = \frac{1}{2}I\Phi_0, \quad (1)$$

where  $I$  and  $\Phi_0$  denote a current surrounding a macroscopic boson and a magnetic flux of a macroscopic boson having the unique value. The fact of the presence of this persistent current  $I$  can be cited from [12].

In this equation, the magnetic flux is assumed to be quantized because each angular momentum is conserved as mentioned.

$$\Phi_0 = \frac{h}{e}, \quad (2)$$

where  $h$  and  $e$  denote the Planck constant and the charge of a hole. Note that this paper employs both the constant  $h$  and  $\hbar$  as Planck constant.

In this current, the cyclotron angular frequency is introduced.

$$I = \frac{e}{T} = 2\pi e\omega_c = 2\pi e \frac{eB_0}{m} = 2\pi e^2 \frac{\mu_0 H_0}{m}, \quad (3)$$

where  $\omega_c$ ,  $B_0$ , and  $u_0$  denote the cyclotron angular frequency, the constant and unique value of magnetic field in a macroscopic boson, and the magnetic permeability in the vacuum, respectively.

Thus, eq. (1) becomes

$$U = \frac{1}{2} 2\pi e^2 \frac{\mu_0 H_0}{m} \frac{h}{e}, \quad (4)$$

where

$$H_0 = \frac{h}{e} \frac{1}{\mu_0 \pi \eta^2}, \quad (5)$$

where  $\eta$  is the approximated radius of a macroscopic boson.

Because the magnetic field  $B_0$  is expressed as eq. (5), the rest energy, i.e. the mass of a macroscopic boson is formed as,

$$2U = \pi e^2 \frac{\mu_0}{m} \frac{h}{e} \frac{1}{\mu_0 \pi \eta^2} \frac{h}{e} = \frac{h^2}{m \eta^2}. \quad (6)$$

Let us consider the spin of a macroscopic boson to obtain partition function, which creates all the anomaly metal properties.

As mentioned, when a macroscopic boson is created, a complete 2-dimensional motion can be considered. That is, among the x-y-z axes, we cannot consider z-components. Therefore, using W. Pauli matrix, this case considers only x-and y-components.

$$s_x = \frac{\hbar}{2} \begin{pmatrix} 0 & 1 \\ 1 & 0 \end{pmatrix}. \quad (7-1)$$

$$s_y = \frac{\hbar}{2} \begin{pmatrix} 0 & -i \\ i & 0 \end{pmatrix}, \quad (7-2)$$

where  $i$  denotes the imaginary unit.

In this paper, a spin angular momentum is defined as the determinant from W. Pauli matrix.

Thus, each determinant is

$$\det s_x = -\frac{1}{2} \hbar, \quad (8-1)$$

$$\det s_y = \frac{1}{2} \hbar. \quad (8-2)$$

Therefore, a net spin angular momentum of a macroscopic boson is calculated as

$$s \equiv \det s_x + \det s_y = 0 \cdot \hbar. \quad (9)$$

The above result implies that, although a single hole behaves as a fermion, this macroscopic boson behaves like a boson. Thus, the name of this particle is derived from this fact.

Due to the fact that a macroscopic boson follows the Bose's partition function, first we simply consider

$$f_r = \frac{1}{\exp\left(\frac{E_i - E_F}{k_B T}\right) - 1}, \quad (10)$$

where  $E_i$ ,  $|E_F|$ ,  $k_B$ , and  $T$  denote energy, a chemical potential, the Boltzmann constant, and temperature, respectively.

An important point is that the exponential function is approximated as a Maclaurin series,

$$f_r \approx \frac{1}{\frac{E_i - E_F}{k_B T} + 1 - 1} = \frac{k_B T}{E_i - E_F}. \quad (11)$$

This above partition function is very important because all properties in the anomaly metal phase in CuO<sub>2</sub>-based superconductors are described by this partition function. We will see how this equation describes properties of the anomaly metal phase later.

Moreover, this equation has another expression. In semiconductor physics, the following equation holds generally:

$$E_F = E + k_B T \ln\left(\frac{2N_A}{n_i}\right), \quad (12)$$

where  $N_A$  denotes accepter concentration. The number 2 is attached because of the presence of spin.

Moreover,  $\frac{2N_A}{n_i}$  implies doping parameter. Therefore, because  $n_i$  implies concentration of lattices, the

doping parameter is less than the value of the number 1 as long as we consider the picture which holes are doped in a Mott-insulator.

Using the equation above, the partition function, eq. (11), is translated as

$$f_r = -\left[\ln\left(\frac{N_A}{n_i}\right)\right]^{-1}. \quad (11-2)$$

Let us calculate pseudo gap energy, which is directly related to the mass of a macroscopic boson.

First, here, we define carrier concentration of macroscopic bosons considering 2-dimensional energy state density.

$$D_2(E) = \frac{m}{\pi \hbar^2} \equiv p_0, \quad (13)$$

$$n = \frac{1}{d} \int D_2(E) f_r dE, \quad (14)$$

where  $D_2(E)$ ,  $n$ , and  $d$  denote energy state density in 2-dimension, particle concentration, and width of the 2-dimensional sheet, respectively. An important point to note is that the parameter  $d$  [m] is consistently substituted by the number 1 but the reason of the appearances in some equations are to clarify the meaning of these equations.

The integral for concentration (14) is simply conducted as follows, because energy state density in 2-dimension is constant as indicated in Eq. (13) and because partition function  $f_r$  is represented by eq. (11-2). In the process of this calculation of eq. (14), an energy  $E_0$  appears as

$$E_0 = -\frac{d}{p_0} n_0 \times \ln\left(\frac{2N_A}{n_i}\right), \quad (15)$$

This energy  $E_0$  is assumed to be essentially equal to pseudo gap energy. Combined with the mass of a macroscopic boson, this pseudo gap energy is represented as follows:

$$E_0 = -U \times \ln\left(\frac{2N_A}{n_i}\right) = -\frac{1}{2} \frac{\hbar^2}{m\eta^2} \ln\left(\frac{2N_A}{n_i}\right). \quad (16-1)$$

The above derived pseudo gap energy equation has a coefficient for doping function  $\ln$ . This factor is identical to the zero-point energy:

$$\frac{1}{2} \hbar\omega = \frac{1}{2} \frac{\hbar^2}{m\eta^2}. \quad (16-2)$$

However, this derived energy  $E_0$  implies merely a potential. In general, an energy gap appears or disappears involving a photon's emission or absorption. This fact implies that, for a potential to become a general energy gap, the potential is given the product of the fine-structure constant  $\alpha$ , which includes characteristic impedance  $Z_0$  for electromagnetic waves.

Typically, the fine-structure constant  $\alpha$  is given as

$$\alpha = \frac{Z_0 e^2}{4\pi\hbar} = \frac{1}{137.0}. \quad (17)$$

In eq. (17), the impedance  $Z_0$  works as the specific impedance to electromagnetic waves.

Thus, the net pseudo gap energy  $|\Delta|_0$  is derived as follows, which will give the temperature of pseudo gap  $T^*$  as discussed later.

$$|\Delta|_0 = -\frac{1}{2} \frac{\hbar^2}{m\eta^2} \alpha \times \ln\left(\frac{2N_A}{n_i}\right). \quad (18)$$

## 2.1 Calculations to obtain formulas for $T^*$ and $T_0$

Let us calculate the formula of pseudo gap temperature  $T^*$ .

In our previous paper [1], an energy gap is assumed to be proportional to the product between critical temperature  $T_c$  and Fermi energy  $E_F$ . Starting this assumption, the calculation process through substituting an equation of Fermi energy and giving critical temperature reach the following equation.

$$T = -\frac{|\Delta|^2}{k_B^2} \frac{1}{T_c \ln\left(\frac{2N_A}{n_i}\right)}, \quad (19)$$

where  $T_c$  and  $\Delta$  denote critical temperature and a general energy gap, respectively.

This equation generally implies the relationship between a temperature and an energy gap including critical temperature  $T_c$ . When the previously derived energy gap from a macroscopic boson is substituted with an energy gap in the above equation, then variable temperature  $T$  must become a constant of pseudo gap temperature  $T^*$ . Therefore, the temperatures  $T_c$  and  $T^*$  have a dependent relationship. As discussed later, note that this dependent relationship is a different point for the temperature  $T^*$  and  $T_0$ , because  $T_0$  provides the transition temperature in appearance of anomaly metal phase. Thus, as a formula of pseudo gap temperature  $T^*$ , the following equation holds:

$$T^* = -\frac{1}{k_B^2} \frac{1}{4} (3.4 \times 10^{-21})^2 \left[ \ln\left(\frac{2N_A}{n_i}\right) \right]^2 \frac{1}{T_c} \frac{1}{\ln\left(\frac{2N_A}{n_i}\right)} = -\frac{1}{k_B^2} \frac{1}{4} (3.4 \times 10^{-21})^2 \left[ \ln\left(\frac{2N_A}{n_i}\right) \right] \frac{1}{T_c}, \quad (20)$$

where, to the equation of  $|\Delta|_0$  of eq. (18) in creating eq. (20), each physical parameter was substituted. That is, the physical parameters  $m$ ,  $h$ , and  $\alpha$  in eq. (18) were given actual values. Note that radius  $\eta$  is approximated as 1 nm.

In the present paper, we consider the anomaly metal phase properties in  $\text{CuO}_2$ -based superconductors. These properties are determined mainly by the transition temperature  $T_0$ , which is directly related to appearances of the Hall-effect coefficient  $R_H$ . As mentioned, this transition temperature also implies the transition for appearance of the anomaly metal phase. To obtain an equation for the temperature  $T_0$ , we consider derivations of the Hall-effect coefficient  $R_H$ . The Hall-effect coefficient  $R_H$  depends on absolute of energy  $-uB_e$ , where  $u$  and  $B_e$  denote self-magnetic moment of a macroscopic boson and applied magnetic fields, respectively. The absolute of energy  $-uB_e$  involves Boltzmann statistics and thus it is related to concentration (i.e., the number) of macroscopic bosons. Considering these facts, at first concentration of macroscopic bosons is again taken and secondary self-magnetic moment of a macroscopic boson are calculated. In the previously appeared concentration eq. (14), the calculation for energy integral, in turn, is conducted actually because we attempted to obtain temperature  $T$  dependence for  $R_H$

$$n = k_B T \frac{1}{d} p_0 \int_a^b \frac{dE}{E - E_F} = k_B T \frac{1}{d} p_0 \times \ln\left(\frac{T_0}{T_c}\right), \quad (21)$$

where

$$a = k_B T_c \quad b = k_B T_0 \quad . \quad (21-2)$$

Note that the second form of  $f_r$  in eq. (11-2) is not employed here. This obtained concentration  $n$  for macroscopic bosons will be employed later.

In turn, a magnetic moment  $u$  is generally defined as

$$\mu = IS, \quad (22)$$

where  $I$  and  $S$  denote the self-current and the area in which a magnetic flux is presented.

Seeing the schematic Fig.1 of a macroscopic boson (which assumes the motion of a hole to be a circle) and because a magnetic flux of it should be quantized as  $h/e$ , the magnetic flux of a macroscopic boson is

$$\Phi_0 = B_0 \pi \eta^2 \equiv \frac{h}{e}, \quad (23)$$

where radius  $\eta$  is approximated on a cell of the  $\text{CuO}_2$  surface. That is,

$$\eta \approx 1 \text{ nm} \quad (24)$$

Moreover, assuming that a magnetic field among a macroscopic boson is equal to the central magnetic

field generated by a moving hole, a persistent current  $I$  in a magnetic moment is calculated as

$$I = \frac{1}{\mu_0} 2\eta B_0. \quad (25)$$

Consequently, a magnetic moment  $u$  is derived as

$$\mu \approx \frac{2}{\mu_0} \eta \frac{h}{e} \frac{h}{e\pi} \times 10^{18}. \quad (26)$$

Now we begin to calculate RH.

As mentioned, considering an energy  $-uB_e$ , the Boltzmann statics is represented as

$$n = n_0 \exp\left(-\frac{\mu B_e}{k_B T}\right), \quad (27)$$

where  $n_0$  is concentration with no applied magnetic field  $B_e$ .

In this equation, the exponential function is approximated by the Maclaurin series.

$$n \approx n_0 \left(1 - \frac{\mu B_e}{k_B T}\right). \quad (28)$$

In this equation, the previously calculated concentration  $n$ , eq. (21), is applied.

$$k_B T \frac{p_0}{d} \times \ln\left(\frac{T_0}{T_c}\right) = n_0 \left(1 - \frac{\mu B_e}{k_B T}\right). \quad (29)$$

Solving this equation for  $n_0$  and employing the general definition of RH, we reach an important equation.

$$R_H = \frac{\frac{\mu B_e}{k_B T} - 1}{e k_B T \frac{p_0}{d} \times \ln\left(\frac{T_0}{T_c}\right)}. \quad (30)$$

Composition of this equation presents a new temperature  $T_0$ , which implies the appearance of RH.

$$T_0 \equiv \frac{\mu B_e}{k_B}. \quad (31)$$

In turn, let us consider the above definition equation  $T_0$  (the derived formula of RH will be considered again later). While an applied magnetic field  $B_e$  in the definition of  $T_0$  is variable, the magnetic field  $B_0$  is a constant derived by the physical constants. This fact allows us to introduce a variable quantum number  $N$  between  $B_e$  and  $B_0$

$$B_0 = N B_e. \quad (32)$$

Moreover, this variable integer  $N$  is undergone by partition function  $f_r$ .

$$N = N_0 f_r, \quad (33)$$

where eq. (11-2) is applied as  $f_r$ .

Note that the magnetic field  $B_0$  was calculated from eq. (23). This employment of partition function  $f_r$  implies that an application of  $B_e$  makes every direction of some magnetic moments of macroscopic bosons the same orientation. In other words, prior to the application of  $B_e$ , the directions of self-

magnetic moments of each macroscopic boson are random (i.e., up- or down-direction), despite that the conservations of angular momentum produces macroscopic bosons. But the application of  $B_e$  presents all the directions of some magnetic moments of macroscopic bosons with the same orientation. Because the interaction between macroscopic bosons with the same directed magnetic moment is repulsive, these bosons now obtain the existences as single and independent particles. Assembling these facts, the conclusive equation of the transition temperature  $T_0$  is derived, which depends on carrier doping.

$$T_0 \approx -\frac{2}{\mu_0 e} \times 10^{-9} \frac{1}{k_B e \pi} \times 10^{18} \frac{1}{N_0} \times \ln\left(\frac{2N_A}{n_i}\right). \quad (34)$$

As described later, this equation of  $T_0$  and the formula of critical temperature  $T_c$  [1] will be crucial factors when calculating properties of the anomaly metal phase.

### 2.3 Analyze anomaly metal phase

Next, we derive dependences on temperature of RH. Up to the previous section, the general equation of RH was derived, which resulted in a definition of transition temperature  $T_0$ . In this equation, we introduce the following approximation to the general equation of RH.

$$\frac{\mu B_e}{k_B T} \gg 1. \quad (35)$$

According to this approximation, the general equation of RH becomes as

$$R_H \approx \frac{\mu B_e}{e(k_B T)^2 \frac{p_0}{d} \times \ln\left(\frac{T_0}{T_c}\right)}. \quad (36)$$

Thus, the approximated equation of RH is determined by applied magnetic fields  $B_e$ . That is, this RH equation depends on both quantum number  $N$  and the universal magnetic field  $B_0$ .

$$R_H \approx \frac{\mu B_0}{e(k_B T)^2 \frac{p_0}{d} \times \ln\left(\frac{T_0}{T_c}\right)} \frac{1}{N}. \quad (37)$$

Note that the universal magnetic field  $B_0$  is one in a macroscopic boson. Thus, in view of magnetic field energy, an application of magnetic field which dominates over the universal magnetic field  $B_0$  results in destructions of macroscopic bosons and makes the anomaly metal phase disappear. Moreover, the employment of quantum number  $N$  implies that the RH equation is determined by doping. That is, variable integer  $N$  is expressed by partition function  $f_r$ , which also implies doping.

$$\frac{1}{N} = \frac{1}{N_0 f_r} = -\frac{1}{N_0} \times \ln\left(\frac{2N_A}{n_i}\right). \quad (38)$$

Considering this, the approximated RH equation further becomes

$$R_H \approx -\frac{\mu B_0}{e(k_B T)^2 \frac{p_0}{d} \times \ln\left(\frac{T_0}{T_c}\right)} \frac{1}{N_0} \times \ln\left(\frac{2N_A}{n_i}\right). \quad (39)$$

As many literatures reported [18], this derived equation of RH is proportional to  $(\frac{1}{T})^2$ .

In Result section, we will depict this RH equation in terms of both doping parameters and temperatures T.

In turn, let us consider electron specific heat coefficient in the anomaly metal phase. Because electron specific heat coefficient is essentially equal to average energy U contributed by macroscopic bosons, it is simply necessary to calculate the average energy using partition function fr. Thus, average energy using partition function fr for energy integrals is given as

$$U = \frac{\int E f_r dE}{\int f_r dE}. \quad (40)$$

Note that the lower limitation a and the upper limitation b of these integrals are given as

$$a = k_B T_c \quad b = k_B T_0. \quad (41)$$

Assuming the Fermi energy for macroscopic bosons (i.e., the chemical energy, but not for single holes) is sufficiently small, the calculation results in

$$U = \frac{k_B T_0 - k_B T_c + E_F \times \ln(\frac{k_B T_0 - E_F}{k_B T_c - E_F})}{\ln(\frac{k_B T_0 - E_F}{k_B T_c - E_F})} \approx \frac{k_B (T_0 - T_c)}{\ln(\frac{T_0}{T_c})}. \quad (42)$$

In general, electron specific heat coefficient is derived by differential in terms of temperature to the average energy. In the present paper, however,  $\Delta T$  is employed, instead of the differential for temperature. Moreover, this  $\Delta T$  is assumed to be  $(T_0 - T_c)$  in this paper. Therefore, using the average energy of a macroscopic boson U and  $\Delta T$ , electron specific heat coefficient is expressed as a calculation process.

$$\gamma_0 = \frac{U}{(\Delta T)^2} = \frac{k_B}{T_0 - T_c} \frac{1}{\ln(\frac{T_0}{T_c})}. \quad (43)$$

Furthermore, to obtain electron specific heat coefficient with the unit [J/mol K<sup>2</sup>], the Avogadro constant  $N_0^A$  is considered here because previously calculated average energy U implies one for a macroscopic boson. Consequently, electron specific heat coefficient is derived as

$$\gamma = \frac{N_0^A k_B}{T_0 - T_c} \frac{1}{\ln(\frac{T_0}{T_c})}. \quad (44)$$

#### 2.4 Superconductivity with consideration of many-body interactions

In the previous section, mainly anomaly metal properties were described. However, it is necessary to describe why macroscopic bosons undertake Bose-Einstein (BE) condensation by forming a pair from two macroscopic bosons, despite that they have been already general bosons such as Cooper pairs. In the previously published paper [1], we found a new attractive force to combine particles from local current in a CuO<sub>2</sub> cell [12]. Because this local current is equal to rotational and self-current which

creates the mass of a macroscopic bosons; hence, this result of the previous paper thus agrees with the descriptions in the present paper. Therefore, in this section, based on the understanding that two macroscopic bosons form a pair, we describe why BE condensation occurs in so high temperature, with consideration of many-body interactions between the bosons.

There are many-body interactions in terms of carriers in various materials. Especially, this fact is essential to high-T<sub>c</sub> cuprates, because the general band theory cannot be applied. The many-body interactions of carriers imply there are many local temperatures  $T_i$  in the materials, where  $i$  is index for a location. In other words, in a temperature  $T_i$ , thermal equilibrium can be assumed. Thus, Fig. 2 indicates our model to handle many-body interactions. In this figure, a radius  $a_i$  forms a sphere shell, which has differential number  $dN$  and local temperature  $T_i$ . Moreover, in the center, a macroscopic boson is presented. The immediately outer particles out of  $dN$  give a pressure to this sphere shell, which equals to kinetic energies of particles in  $dN$  (i.e., it is represented by a temperature  $T_i$ ), while the central macroscopic boson provides force of thermal expansion, which implies electrostatic energy, i.e., Coulomb interactions. Moreover, the present case adds magnetic interactions between macroscopic bosons as a force of thermal expansion.

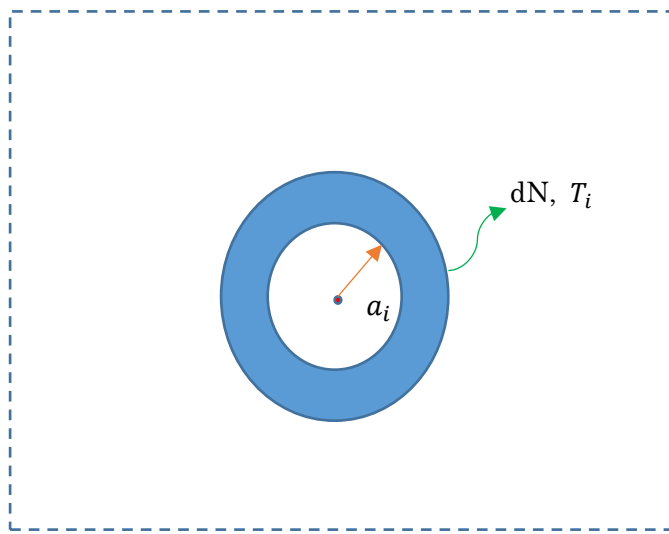


**Fig.2**

**Schematic of our established model to handle many-body interactions.** Considering a nature of many-body interactions, it is important to note that temperatures are locally different. However, this model claims that in differential number  $dN$  (a macroscopic boson takes the center and  $dN$  takes a temperature  $T_i$ ), thermal equilibrium can be assumed. Considering this, a proportion between force of thermal expansion from Coulomb interactions in addition to the magnetic field interactions from the bosons and force of compression from immediate outer side, which is equal to the kinetic energies in  $dN$  (i.e., a temperature  $T_i$ ), is formed. Calculating this proportional equation results in a new statistic equation.

Considering that these forces of thermal expansion should be proportional to a force of compression in a sphere shell, the following relation holds:

$$(\text{Coulomb interaction energy and magnetic field interaction energy}) = \frac{3}{2} k_B T_i \times dN$$

Calculate this equation.

First,  $dN$  is represented as

$$dN = g f d\vec{k} = g f \left(\frac{1}{dV}\right), \quad (45)$$

where  $k$ ,  $V$ ,  $g$ , and  $f$  denote wave number, volume, state number, and partition function for the boson, respectively.

In the equation of  $dN$ , as mentioned, state number  $g$  and partition function  $f$  are given as

$$f \equiv f_r = -[\ln(\frac{2N_A}{n_i})]^{-1}. \quad (46)$$

$$g = \frac{1}{d} \int D_2(E) dE = p_0 E_0, \quad (47-1)$$

$$D_2(E) = \frac{m}{\pi \hbar^2} \equiv p_0, \quad (47-2)$$

$$E_0 = |\Delta|_0 = -\frac{1}{2} \frac{\hbar^2}{m \eta^2} \alpha \times \ln(\frac{2N_A}{n_i}). \quad (47-3)$$

Thus,  $fg$  is given as

$$fg = p_0 \frac{1}{2} \frac{\hbar^2}{m \eta^2} \alpha. \quad (48)$$

To calculate the left-hand side of the above-mentioned proportional equation. The electrostatic energy  $U_E$  is calculated as

$$U_E = \frac{1}{2} \epsilon_0 \left(\frac{e}{4\pi\epsilon_0 a_i^2}\right)^2 dV, \quad (49)$$

where  $\epsilon_0$  and  $a_i$  denote the permittivity for the vacuum and the radius which  $dN$  is taking in the model.

At this time, a volume element of the integral is expressed as

$$dV = \frac{1}{d\vec{k}} = \frac{4\pi}{3} a_i^3. \quad (50)$$

Moreover, the magnetic interaction  $V_p$  from macroscopic bosons is given as

$$V_p = U_B dN, \quad (51)$$

Consequently, the resultant equation is provided by

$$a_i^2 = \frac{9\epsilon_0}{e^2} (3k_B T_i - 2U_B) fg. \quad (52)$$

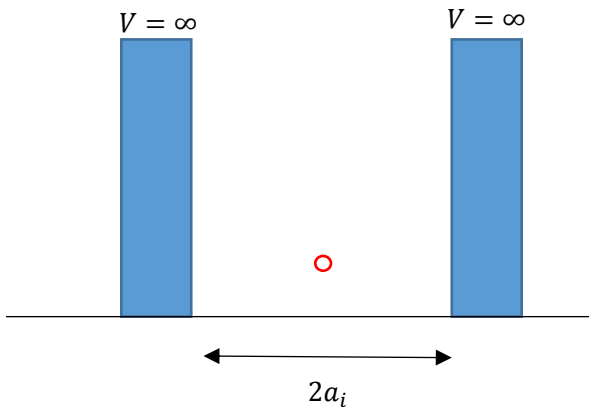


**Fig. 3**

**A basic model of well-potential. This model is directly related to the immediate prior figure model. The diameter  $2a_i$  varies, depending on a temperature  $T_i$ . A macroscopic boson in this well-potential forms a stationary wave, and its wave function and eigenvalue are presented in every basis texts. An important point is that all of these depends on index i.**

As shown in Fig.3, the central macroscopic boson behaves under the model of well-potential. Thus, the eigenvalue and wave function of it are presented by

$$\psi_i(r) = \sqrt{\frac{2}{2a_i}} \sin\left(\frac{i\pi r}{2a_i}\right). \quad (53)$$

$$E_i = \frac{\hbar^2 i^2 \pi^2}{2M \times 2a_i}, \quad (54)$$

where M, i, and r denote the mass of a macroscopic boson, index, and microscopic variable of sphere-coordinates, respectively.

These equations imply that a particle under the many-body interactions forms a stationary wave and that the wave function of the stationary wave and the eigenvalue (i.e., kinetic energy) are determined by a radius  $a_i$ .

Using the above concept, we consider how BE condensation occurs. Besides a sphere shell having temperature  $T_i$ , another sphere shell having temperature  $T_j$  is considered here. When we accept a combination of two macroscopic bosons by a force F, these two bosons must have the identical kinetic energy because, in general and as mentioned in our previous paper [1], a relative and attractive force appears only when their relative velocities become the same. In particular, that fact is applied when the attractive Lorentz force generates between moving and charged particles whose velocities are identical. Thus, when forming a pair from two macroscopic bosons, the eigenvalues indexed by i and j becomes equal. That is,

$$|E_i - E_j| = 0, (55)$$

This implies that an index  $i$  and  $j$  becomes equal, resulting in that all the radius  $a_i$  and eigenvalue  $E_i$  take the identical radius  $a_0$  and  $E_B$ , because of the arbitrary property of index  $i$ . Hence, if a pair forms, every energy of macroscopic bosons undergoes the identical energy  $E_B$ , which implies these bosons take BE condensation.

Moreover, as shown in Fig. 4, taking index  $i$  to be equal  $j$  implies that temperatures  $T_i$  and  $T_j$  must be equal. Even at this moment, positions  $r$  of wave functions, eq. (53), are common and thus the two sphere shells take the superposition, i.e. the relative distance  $\xi_G$  between the two sphere shells should be zero and the combination is now formed. Thus, the net coherence of two holes becomes on a cell order, 1 nm, as reported by many literatures.

Employing the above-mentioned equation (52), an equation of the relative distance between sphere shells  $\xi_G$  for temperature  $T$  is derived as follows:

$$\frac{1}{4} \xi_G^2 = \frac{9\varepsilon_0}{e^2} (3k_B \langle T \rangle - 2U_B) g f, (56)$$

where  $U_B$  is substituted with pseudo gap  $|\Delta|_0$  in eq. (18).

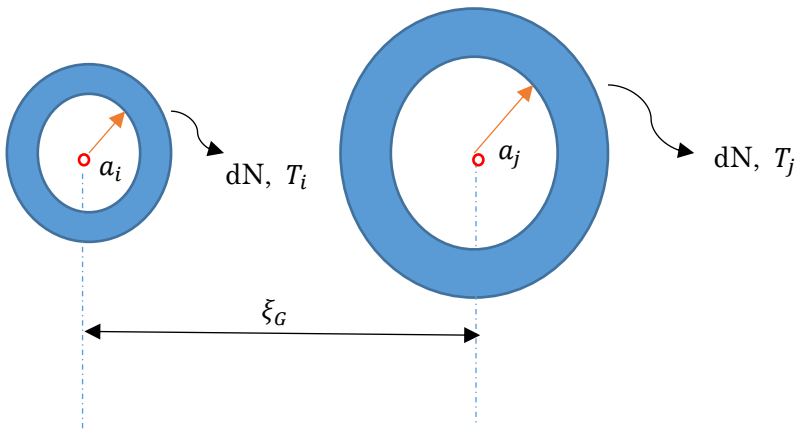


Fig. 4

**Schematic of two macroscopic bosons having many-body interactions. The relative distance of  $\xi_G$  implies one between two macroscopic bosons. When an attractive force  $F$  between them appears and because the relative kinetic energy becomes zero, indexes  $i$  and  $j$  take the same. Thus, a superposition between them occurs, rendering  $\xi_G$  be zero. That is, two bosons now combine to be a Cooper pair. Employing the statistic equations from our established model, we can predict this type of transition.**

As will be discussed in Result section, temperatures at which  $\xi_G^2 \leq 0$  implies superconductivity state (i.e., the net coherence of two holes is about 1 nm, which equals CuO<sub>2</sub> cell order) and the transition temperature  $T_c$  at which  $\xi_G = 0$  implies a critical temperature.

## 2.5 Review to obtain the formula for $T_c$

Let us review our previous paper [1], which describes a force  $F$  to combine two particles and a critical temperature on doping.

Note that because this is a review to understand the stream of outlined derivations of a critical current  $T_c$ , some equations in the calculation process and derivation process are left out. In case that the reader is interested in the detail, the paper can be downloaded the paper as an Open Access paper.

First, we assume that a general energy gap is proportional to both Fermi energy and Critical current as follows:

$$|\Delta|^2 = k_B T_c E_F, \quad (57)$$

In this equation, the fermi energy in a p-type material is employed as,

$$p : E_F = E_i - k_B T \log\left(\frac{2N_A}{n_i}\right), \quad (58)$$

In this equation, a superconducting energy gap is introduced.

$$2E_i = k_B T_c, \quad (59)$$

Substituting these energies and employing the state equation with the universal gas constant  $R$ , the following equations are obtained.

$$|\Delta|^2 = \frac{1}{2} (k_B T_c)^2 \left\{ 1 - 2 \frac{T}{T_c} \log\left(\frac{2N_A}{n_i}\right) \right\}, \quad (60)$$

and

$$|\Delta|^2 = \frac{1}{2} (k_B T_c)^2 \left\{ 1 - 2 \frac{1}{T_c} \frac{|\Omega_B|}{R} \frac{1}{2N_A} \log\left(\frac{2N_A}{n_i}\right) \right\}, \quad (61)$$

where

$$|\Omega_B| = PV, \quad (62)$$

where  $\Omega_B$  denotes a thermodynamic potential.

In this way, a general expression of energy gap for temperatures is derived.

Next, let us consider the derivation of superconducting energy gap.

To consider the superconducting energy gap, it is necessary to mention a force  $F$ , which results in a combination of a Cooper pair. As mentioned previously, two charged particles generally experience an attractive force with each other when they are moving with the same velocity, i.e., when the relative energy or momentum is zero. As shown in Fig. 5-1 to 5-4, at first two parallel conductors along which

the same direction and same amount of a current are presented. From the electromagnetism, these current leads experience an attractive force with each other, which results from the Lorentz force. When we shorten these leads to a wavelength of a carrier, this attractive force still exists. This implies that two charged particles whose wave numbers are identical experience an attractive force with each other.

Considering this fact, a force  $F$  and its energy (i.e. superconducting energy gap) is represented as

$$F = q^2 \frac{\hbar \mu_0}{m^2} \frac{4\pi^2}{k^2} |\Psi|^2 k^2 \frac{1}{2r} \sin \theta \cos \phi = \frac{2q^2 \pi^2 \mu_0 \hbar}{m^2} |\Psi|^2 \frac{1}{r} \sin \theta \cos \phi \quad (63)$$

$$u = -\frac{2q^2 \pi^2 \mu_0 \hbar}{m^2} \beta |\Psi|^2 \log r \sin \theta \cos \phi + u_0 \quad u_0 \leq 0 \quad , \quad (64)$$

where  $\psi$ ,  $r$ ,  $\theta$ ,  $\phi$ ,  $q$ ,  $\beta$ , and  $u_0$  denote wave function of a hole, relative distance of two holes, angle associated with the Lorentz force, angel related with two wave number of holes, the electric charge of a hole, constant, and integral constant, respectively.

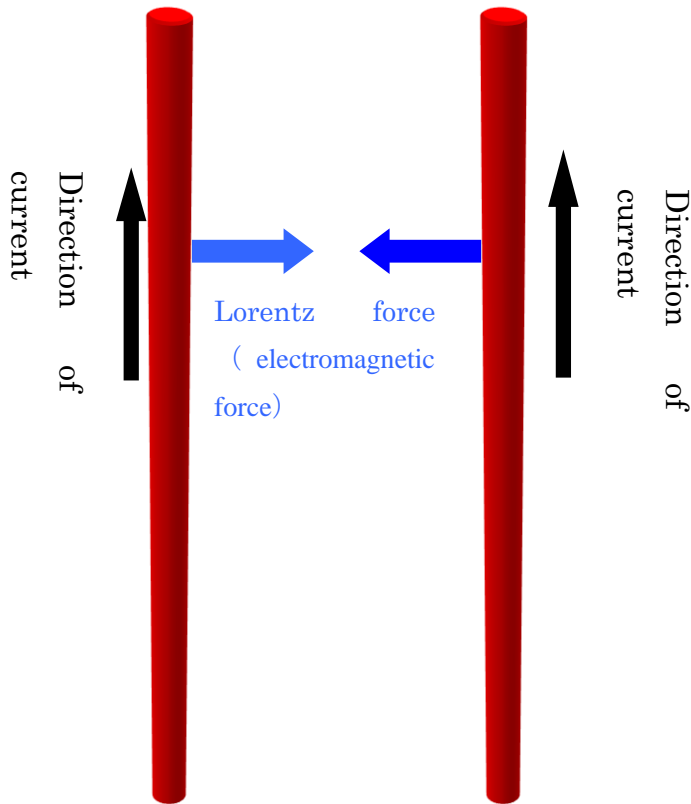


Fig. 5-1: Currents in the same direction. Note that this figure was cited from [1]

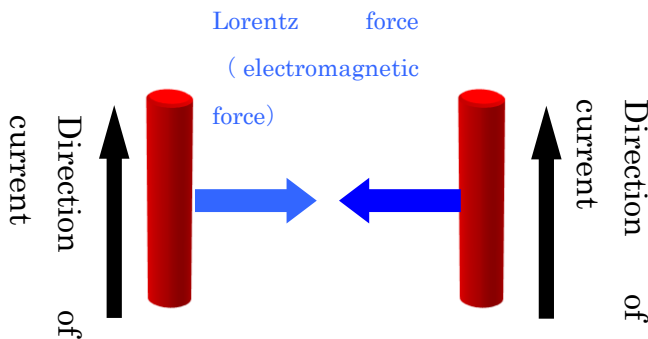


Fig. 5-2 Shorter leads with currents in the same direction. Note that this figure was cited from [1]

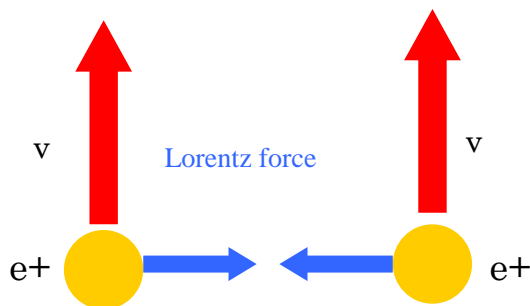


Fig. 5-3 Holes with same direction and equal velocity. Note that this figure was cited from [1]

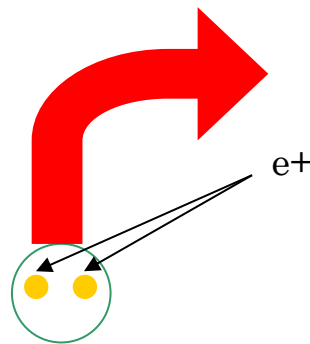


Fig. 5-4 Center-of-mass motion of Cooper pair. Note that this figure was cited from [1]

Furthermore, the derived superconducting energy gap  $u$  is given a relationship with the pseudo gap energy.

$$T_c = -4\alpha'^2 \frac{|\Omega_B|}{R2N_A} \log\left(\frac{2N_A}{n_i}\right) - 1.14\theta_D, \quad (65-1)$$

where

$$\alpha = -\frac{2q^2\pi^2\mu_0\hbar}{m^2} \log \xi \sin \theta \cos \phi \quad (65-2)$$

$$\alpha' = \eta\alpha = -\frac{1}{k_B\theta_D} \alpha = -\frac{1}{k_B\theta_D} \frac{2q^2\pi^2\mu_0\hbar}{m^2} \log \xi \sin \theta \cos \phi \quad (65-3)$$

In this process, we added a Debye temperature  $\theta_D$  and a net coherence  $\xi$  to the equation. Note that, as an integral constant, the BCS formula under a particular condition was employed. That is, in the formula  $T_c$  of BCS theory, because the interaction potential  $V$  in the BCS formula equals the mass of a Cooper pair and when the mass of a macroscopic boson  $U$ , eq. (6), is substituted to  $V$  in the BCS formula, in turn, this large value of  $U$  makes the exponential function in the BCS formula zero.

Concerning the thermodynamic potential, the following equation is applied under the condition of BE condensation.

$$|\Omega_B| = PV = \frac{2}{5}E_{F0}, \quad (66-1)$$

$$2E_{F0} = E_{G0}, \quad (66-2)$$

where  $E_F$  and  $E_G$  denote the Fermi energy and band gap at zero temperature, respectively.

Thus, critical temperature becomes

$$T_c = -4\left(\frac{1}{k_B\theta_D}\right)^2 \left(\frac{2q^2\pi^2\mu_0\hbar}{m^2} \log \xi \sin \theta \cos \phi\right)^2 \frac{E_G}{5R2N_A} \log\left(\frac{2N_A}{n_i}\right) - 1.14\theta_D. \quad (67)$$

Moreover, we derive 2-dimensional critical temperature equation from the above.

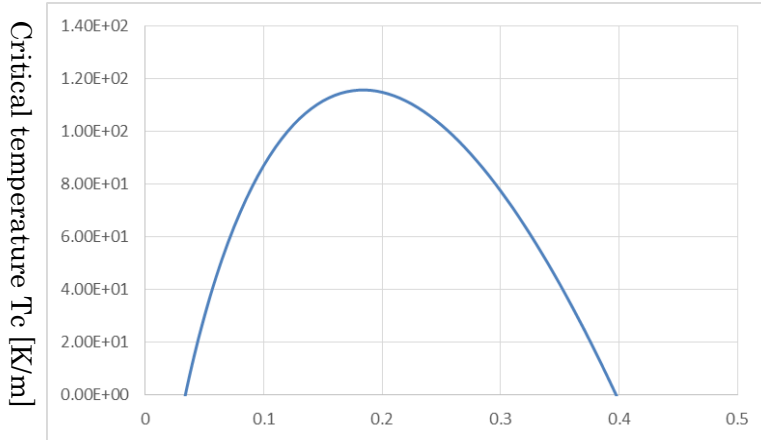


Fig.6

doping

A result of typical critical current on doping. This is derived from the equation by combining pseudo gap energy and superconducting energy gap. At doping 0.16, the critical temperature reaches the maximum, which agrees with the experiments. In calculations, no numerical calculations or fitting method are employed. The values of critical temperatures are relatively sensitive for Debye temperature and band gap in our derived equation. This

implies that, although high-Tc cuprates in common have CuO<sub>2</sub> surfaces, differences of Debye temperatures and band gaps would result in various values of critical temperatures among high-Tc cuprates.

Thus, to conclude, a critical temperature equation is derived as

$$\langle T_c \rangle_2 = -4\left(\frac{1}{k_B\theta_D}\right)^2 \left(\frac{2q^2\pi^2\mu_0\hbar}{m^2} \log \xi \sin \theta \cos \varphi\right)^2 \frac{E_G n_q}{5R2\sigma} \log\left(\frac{\sigma}{n_{i2}}\right) - 1.14\theta_{D2} \quad [\text{K}/\text{m}], \quad (68)$$

where  $\sigma$ ,  $\theta_D$ , and  $n_q$  denote surface density of carriers and Debye temperature in 2-demention, which is assumed to be approximately equal to that of 3-dimension, and the number of layer.

Note that all the constants in the consequent equation have actual physical meaning and unit. This implies that no numerical calculations or fitting methods are required. This fact is also consistent everywhere in the present paper.

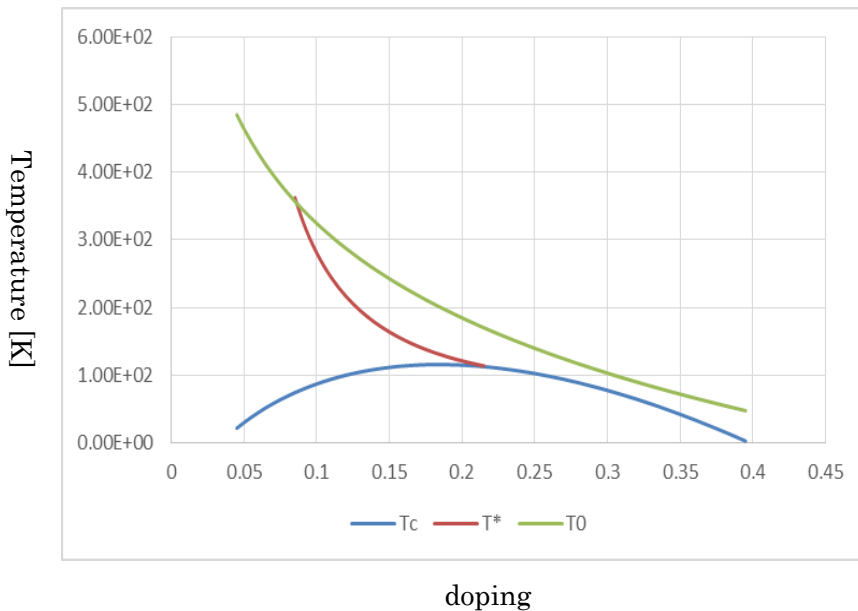
Table 1 Physical parameters in the equation of critical temperature

Debye temperature $\theta_D$	140 K
Coherence $\xi$	1 nm
Band gap $E_G$	$1.53 \times 10^{-18} \text{ J}$
The number of layer $n_q$	3

In Fig.6, a result of this review section is shown, where used physical parameters are listed in Table 1. As shown, our derived critical temperature equation sufficiently agrees with a typical high-Tc copulate. Note that the reason why the band gap is relatively large is related to the property of the Mott-insulator. For the detail, refer to [1].

### 3. Results

First, Fig. 7 shows the entire depictions of  $T_c$ ,  $T^*$ , and  $T_o$  on doping as a result of analytical calculations. Generally, the agreements with the experiments is good. Moreover, in Fig. 8, the result of theoretical calculations of the Hall coefficient  $R_H$ . As shown, the lower doping, the higher  $R_H$ , and the  $R_H$  behave as non-linear on temperatures. This result accurately agrees with the experiments such as [18]. Furthermore, Fig. 9 indicates a result of theoretical calculation for electron specific heat coefficient. According to the experiments [19,20], the calculation values are valid in addition that it takes the maximum at a higher doping.

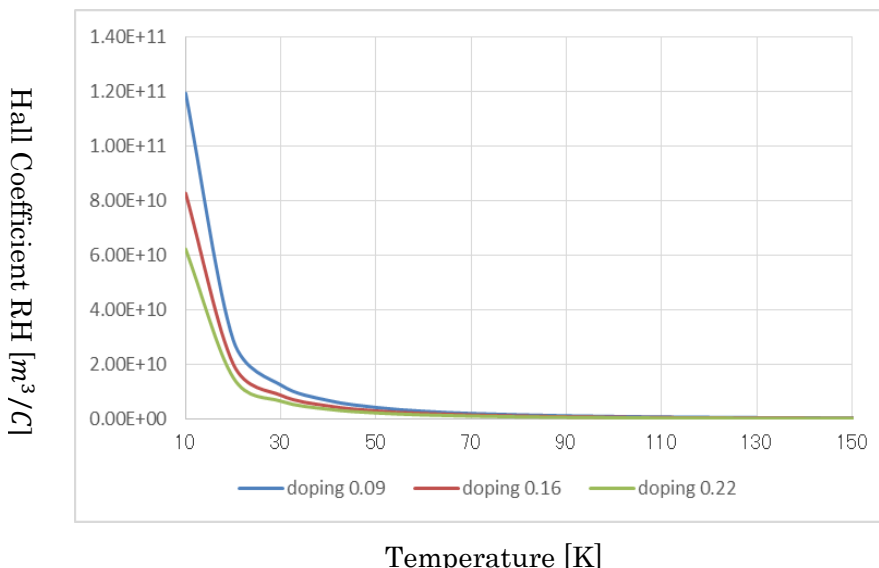


doping

**Fig. 7**

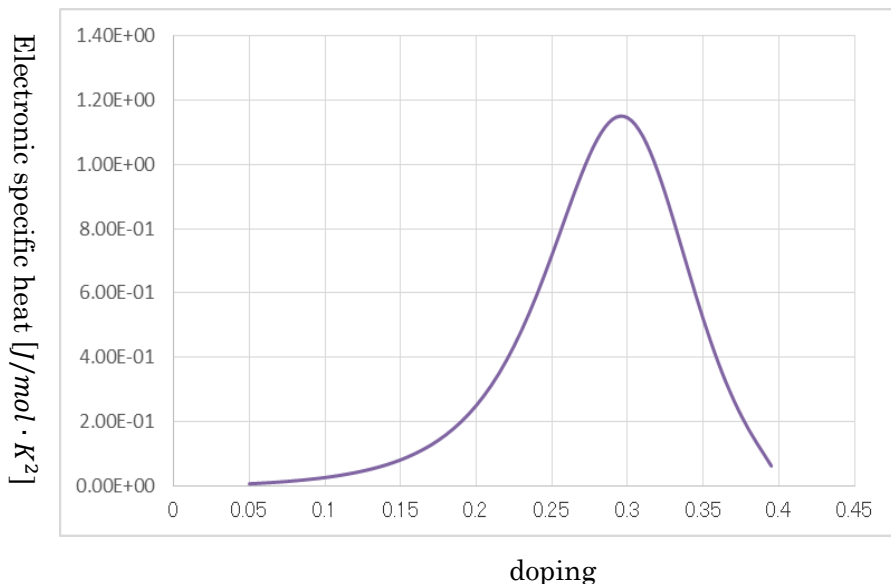
The whole depiction from theoretical calculations of  $T_c$ ,  $T^*$ , and  $T_0$  vs. doping.

For the previous figure of  $T_c$  graph,  $T^*$  and  $T_0$  are added. Note that  $T^*$  is depicted on the understanding that it is smaller than  $T_0$ . Moreover,  $T^*$  has the gradual and easy minimum point on touching  $T_c$  dome. Thus, it does not exist in the  $T_c$  dome. As mentioned, no numerical calculations and fitting methods are employed.  $T_0$  begins with about 500 K and vanishes almost at the same doping at which  $T_c$  disappears. As mentioned in the text, this transition temperature is important in considering the anomaly metal phase.

**Fig. 8**

Hall-effect coefficient RH on both temperature and doping.

As many experimental literatures report, the lower doping takes, the higher RH becomes. The calculated values generally agree with experiments in addition that temperate dependence is non-linear. Note that the quantum number  $N_0$  in RH equation, which varies on the applied magnetic fields  $B_e$ , was assumed to be  $1.1 \times 10^2$ .

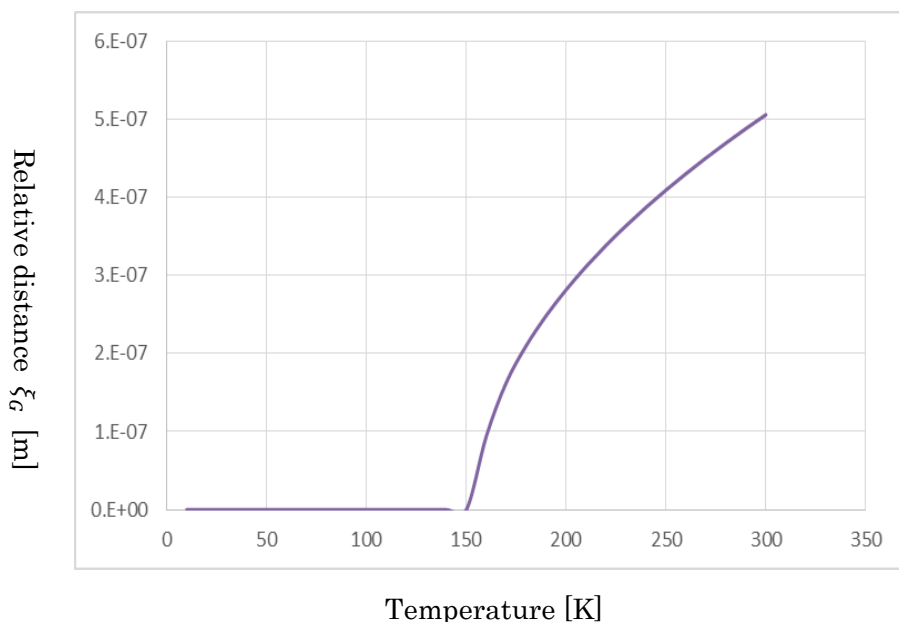


**Fig. 9**

A theoretical result of electron specific heat coefficient on doping.

At the relatively high doping, the curve takes the maximum, which agrees with the experiments. In other words, to both lower doping or higher doping from this the maximum, electron specific heat coefficient decreases.

As a result of the statistic equation for the many-body interactions, Fig. 10 shows superconductivity state up to a critical temperature about 140 K. In this figure, the state, which relative distance  $\xi_G$  between two macroscopic bosons with consideration of the many-body interactions, under zero implies superconductivity state. From the further temperatures higher than the critical temperature, relative distance  $\xi_G$  becomes much larger as a change of non-continuity. Obviously, a transition occurs at around 140 K.

**Fig. 10**

**Relative distance between two macroscopic bosons vs. temperature.** Because up to about 140 K relative distances  $\xi_G$  is not defined according to our statistic equation to handle the many-body interactions, up to about 140 K, the net coherence of two holes is defined as about 1 nm, i.e., superconductivity state is maintained. However, at the further temperatures, relative distances  $\xi_G$  suddenly becomes  $10^{-7} m$  order. Obviously, a transition occurs at around 140 K. As an important notation, the magnetic field interaction  $U_B$  is substituted by the pseudo gap energy at the optimum doping 0.16. Thus, as many researchers claim, the many-body interactions in terms of macroscopic bosons (not holes) is one of the reasons why high-Tc cuprates exhibit so high critical temperate.

## 4. Discussion

### 4.1. Macroscopic boson and high-Tc cuprates

Since the first discovery of a high-Tc cuprate, many experiments have been reported as well as suggested theories. However, according to current researchers' challenges, the mechanism of high-Tc cuprates is yet to be uncovered. At least, researchers in superconductivity do not have the consensus to describe the mechanism behind it.

We propose that the reason behind the challenges of many researchers is that a particle describing high-Tc cuprates is not a normal hole but a macroscopic boson, which is formed by the conservation of angular momentum in 2-dimension and by rotational motion of a hole itself. The concept of a macroscopic boson, as mentioned, provided a unique partition function, and this partition function can explain every property in the anomaly metal phase. Moreover, the presence of this boson

gives substantial reason why high-T<sub>c</sub> cuprates have significantly high critical temperature when considered with many-body interactions

In particular, most important points in high-T<sub>c</sub> cuprates are to understand the nature of force to combine two holes as a Cooper pair and to understand that carriers that contribute to the high-T<sub>c</sub> superconductors are macroscopic bosons (i.e., not single hole), which are created due to the presence of 2-dimensional CuO<sub>2</sub> surface and due to the conservation of angular momentum.

#### 4.2 *Anomaly metal phase and transition temperature T<sub>0</sub>*

Thus far, to understand the mechanism of a high-T<sub>c</sub> cuprate, it was important to study the source of pseudo gap energy. Although this is true, another important factor which should be understood is the source of the transition temperature T<sub>0</sub>, which defines the anomaly metal phase appearance. As mentioned, all the equations which describe the anomaly metal phase have the parameter T<sub>0</sub> as well as T<sub>c</sub>. Therefore, excessive focus on the source of pseudo gap energy made most researchers less careful of the source of the transition temperature T<sub>0</sub>, and this confused researchers when considering the mechanism.

#### 4.3 *Highlights of the process for the materials to undergo superconductivity*

Let us review the process, which describes the mechanism from forming a macroscopic bosons to undergoing BE condensation.

First, high-T<sub>c</sub> cuprate reaches the transition temperature T<sub>0</sub> with a lower or no refrigeration. At this stage, because the wavelength of a hole along z-axis becomes longer than the width of 2-dimensional CuO<sub>2</sub> surface, the net 3-dimension disappears and the conservation of angular momentum forms a macroscopic boson, which implies the rotation of a hole producing a magnetic field energy. Thus, this magnetic field energy gives a mass of macroscopic boson.

By further refrigeration, many-body interactions including the magnetic field energy of macroscopic bosons and Coulomb interactions result in very short relative distance of two holes (i.e., the net coherence of about 1 nm). Simultaneously, two holes gain a strong combination of the Lorentz force, because the relative kinetic energy among two holes becomes zero.

As a result of our established statistic equation, all the Cooper pairs take the identical energy and thus BE condensation is produced, which is the source of the Meissner effect.

#### 4.4 The reason why high-T<sub>c</sub> cuprates have significantly high critical temperature

As mentioned, an attractive force is the Lorentz force when two charged particles have no relative kinetic energy. However, as indicated in Fig. 11, this concept can also be satisfied in s-wave pair as well as d-wave pair. Considering this schematic figure, the pair symmetry of high-T<sub>c</sub> cuprates as d-wave is not important. Rather, it is crucial to focus on an irregular many-body interactions in high-T<sub>c</sub> cuprates with an explanation of the significantly high critical temperature.

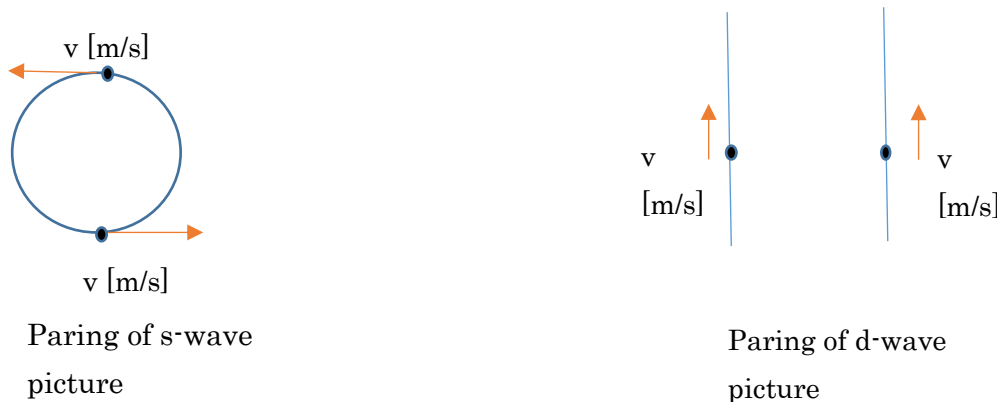


**Fig. 11**

Schematic of paring symmetries.

The principle to generate an attractive force between two charged particles is that relative momentum must be equal. That is, when this principle is satisfied and if outer macroscopic heat energy does not disturb, the two charged particles are combined by the generated attractive force, which stems from the Lorentz force. This proves that this principle is satisfied are illustrated in the figures above, i.e., s-wave and d-wave symmetries. This is why there is another irrelevant particle among force-experiencing two particle. This irrelevant charged particle with different momentum does not experience this attractive force. However, the Coulomb interactions does not have this characteristic.

According to the model we employed to handle many-body interactions in terms of charged particles, it is normally impossible for two particles to take their relative distance shorter than about  $10^{-7}$  m. In this case, however, our employed equation in many-body interactions has magnetic field interaction  $U_B$  in eq. (56) due to the presence of macroscopic bosons (i.e. pseudo gap energy) as well as Coulomb interaction. Therefore, this fact renders relative distance between two macroscopic bosons to be zero up to a high temperature, which makes the net coherence of two holes become the order on the cell of a CuO<sub>2</sub> surface (i.e. about 1 nm).

This is demonstrated as shown in Fig. 10, which results in a critical temperature about 140 K. Considering  $U_B$  in eq. (56) in our model equation to handle many-body interactions is pseudo gap energy, eq. (18), which is essentially equal to the mass of a macroscopic boson, the parameter  $\eta$  [m] (i.e., radius of a boson and order on a  $\text{CuO}_2$  cell) determines the critical temperature as well as doping. This parameter also determines both a Debye temperature and a band gap. Thus, this fact does not contradict the critical current equation (68) in this review section or our previous paper [1].

Furthermore, according to our derived statistic equation, the larger  $U_B$  is, the higher a critical temperature  $T_c$ , and actual high- $T_c$  implies that  $U_B$  is sufficiently large, which results when the parameter  $\eta$  [m] is sufficiently small in addition to the optimum doping.

To conclude, the existence of a macroscopic boson implies that:

- 1) It causes the anomaly metal phase in high- $T_c$  cuprates.
- 2) Irregular many-body interactions are caused by it, which results in a high critical temperature higher than  $\text{LN}_2$ .

Note that, if we consider electron-doping in a Mott-insulator, carrier concentration dominates over the lattice concentration  $n_i$  with consideration of the local electron at each lattice in the Mott-insulator, and thus the sign of the function  $\ln$  in eq. (18) of pseudo gap energy (i.e.,  $U_B$  in eq. (56)) is altered. Hence, the sign of  $U_B$  in eq. (56) also becomes the opposite, which makes electron-doping unable to have a high critical temperature because on the contrary  $U_B$  would prevent the enhancement of critical temperatures  $T_c$ .

#### 4.5 Consideration of significances in this paper

We believe that this paper is significant because:

- 1) It clarified why high- $T_c$  cuprates have actual high critical temperature higher than  $\text{LN}_2$ .
- 2) It showed that all the puzzles including the properties of anomaly metal phase reported in previous articles have been attributed to the presence of a macroscopic boson.

Thus far many theoretical investigations were reported to explain the mechanism of high- $T_c$  cuprates but most of them used numerical computing or fitting methods. However, a general understanding of how the mechanism worked was largely unknown. Therefore, we proposed a detailed explanation of the mechanism which has been proposed for a comprehensive understanding of high- $T_c$  cuprates.

## 5. Conclusion

This paper described theoretically high-Tc cuprate properties such as the transition temperatures on doping, Hall-effect or electron specific heat coefficient on doping. Moreover, it established a novel model to handle general many-body interactions, which explained why the high-Tc cuprates exhibit a significantly high critical temperature.

In general, the derived resultant equations predicted values accurately agree with the data from experimental reports, with no numerical calculations and fitting methods.

The resistivity on lower doping in the anomaly metal phase is not discussed in this paper. However, an equation for conductivity which takes linearly temperature dependence (i.e., non-linearly resistivity) was obtained in the Theory section of the paper, because the carrier concentration in eq. (21), which linearly depends on temperatures, implies the conductivity. However, the non-linearly resistivity in the anomaly metal phase which appears only on low doping and mobility from the experiments is unclear because it is directly related to superconductivity (i.e., resistivity = 0). Therefore, because it does not only involve macroscopic bosons but also magnetic flux quanta and I-V characteristic, the subject is complex. Thus, we expect further investigations on the subject involving magnetic flux quanta and critical current density in the future.

## References

- [1] S. Ishiguri, *Results in Physics*, **3**, 74-79 (2013)
- [2] J.G. Bednorz and K.A. Müller, *Zeitschrift für Physik B*, **64**, 189–193 (1986)
- [3] M. Yamaguchi, et al., *IEEE Transactions on Applied Superconductivity*, **13** (2), 1848–1851 (2003)
- [4] J. Pitel and P. Kovac, *Supercond. Sci. Technol* **10** 847 (1997)
- [5] S. Ishiguri and T. Funamoto, *Physica C* **471**, 333–337 (2011)
- [6] M. Somayazulu, et al, *Phys. Rev. Lett.* **122**, 027001 (2019)
- [7] H. Mukuda, et al, *Phys. Rev. Lett.*, **96** 087001 (2006)
- [8] Y. Kohasaka, et al, *Science*, **315**, 1380 (2007)
- [9] D.N. Basov, T. Timusk, *Review of Modern Phys.*, **77**, 721 (2005)
- [10] M. Le Tacon, et al, *Nature Physics*, **2**, 537 (2006)
- [11] K. Tanaka, et al, *Science*, **314**, 1910 (2006)
- [12] S. Uchida, *Japanese Applied Physics* (institute journal ), **80**(5), 383-386 (2013)
- [13] T. Fujita, *J. Cryogenics and Superconducting Societies of Japan*, **47**,(2), 89-95 (2012)
- [14]. P. W. Anderson, et al, *J. Phys.: Condens. Matter*, **16**(24), R755 (2004)
- [15]. M. Ogata, H. Fukuyama, *Rep. Prog. Phys.*, **71**, (2008)

- [16] D.J. Scalapino, *Phys. Pep.*, **250**, 329 (1995)
- [17] T. Moriya, K. Ueda, *Advances in Physics.*, **49**, 555 (2000)
- [18] M. Sato, *Research on condensed matter physics*, **72**(4), 431-435 (1999)
- [19] J. W. Loram, et al, *Physica C* **162-164**, 498 (1989)
- [20] N. Momono, et al, *Physica C* **233**, 395 (1994)

#### **Additional information**

This paper is not related to any competing interests such as funding, employment and personal financial interests. Moreover, this paper is not related to non-financial competing interesting.

#### **Acknowledge**

We thank Enago ([www.enago.jp](http://www.enago.jp)) for English language Review.

## Appendix

### A1. Introduction and significances of this appendix

The purpose of this appendix is to confirm the proposed new model to handle many-body interactions described in the main text, by applying another physical phenomenon. As an example, we now introduce transitions of ferromagnetic material, i.e., Curie temperatures.

Before conducting an actual calculation, we will briefly discuss some background information to understand significance of this appendix as well as to confirm our established model. Concerning transition phenomena, many literatures have been reported [a1-a6]. In particular, Ising model is the most famous and basic. According to our literature review, however, few articles exist which accurately predicted that the transition temperatures agreed with data of experiments. Moreover, many statistic physics texts claim that the Ising model in 2-dimension provides an equation of transition temperature but no known model in the 3-dimension. If we follow the existing theory, a calculation of transition temperature implies the evaluation of exchange interaction. However, this interaction is quite abstract and thus it difficult to evaluate in every ferromagnetic material. A general formula to determine a transition temperature has not been obtained because partition function with consideration of many-body interactions cannot be calculated mathematically.

In this appendix, using our established model for many-body interactions, we predict the actual values of transition temperatures which sufficiently agree with the experimental values. These calculations do not involve any numerical calculations or fitting methods. Here, we provide a new model for statistic physics considering many-body interactions.

### A2. Predictions of Curie temperatures using our employed model to handle many-body interactions

As shown in Fig A1, a magnetic moment  $\vec{\mu}$  is located in the center of a sphere shell  $dN$  at which the temperature is  $T_i$ . Similar to that of the main text, the following proportional relation holds:

$$(\text{magnetic field interaction from magnetic moments}) = \frac{3}{2} k_B T_i dN \quad (\text{A-1})$$

In this equation, the left-hand side is given as

$$-\vec{\mu} \cdot \vec{B}$$

As every basic text describes, a magnetic field  $\mathbf{B}$  is represented as

$$\vec{B} = -\frac{\mu_0}{4\pi} \left[ \frac{\vec{\mu}}{r^3} - \frac{3(\vec{\mu} \cdot \vec{r})\vec{r}}{r^5} \right], \quad (\text{A-2})$$

where  $r$  is radius of sphere shell  $dN$ .

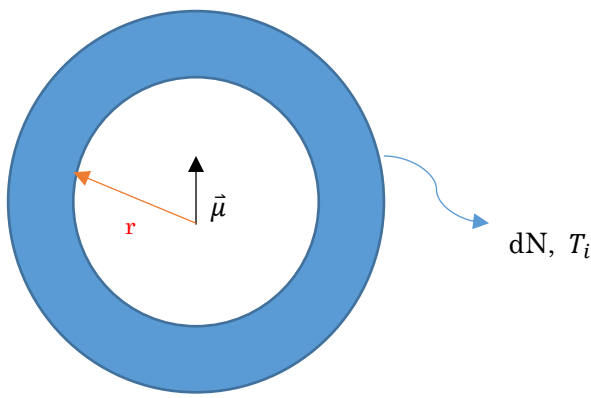


**Fig. A1**

A schematic of our model to apply a ferromagnetic material.

The concept to handle many-body interactions are basically the same as the case presented in the main text. That is, force of thermal expansion from the central magnetic moment  $\vec{\mu}$  is proportional to force of compression from the immediately outer locations, which are equal to kinetic energies in the differential number  $dN$ . Note that, this case does not include the magnetic field interaction by macroscopic bosons. Calculating the proportional equation results in a statistic equation which involves the many-body interactions.

In this equation, the first term implies a ferromagnetic, while the second term is antiferromagnetic. Because the present case is to handle a ferromagnetic material, thus, we employ the first term. Moreover, the directions of two magnetic moments  $\vec{\mu}$  are assumed to be parallel, i.e., the scalar product between two  $\vec{\mu}$  is positive.

Considering the above, the equation becomes

$$-\vec{\mu} \cdot \left[ -\frac{\mu_0 \vec{\mu}}{4\pi r^3} \right] = \frac{3}{2} k_B T_i dN. \quad (\text{A-3})$$

Moreover, as mentioned,  $dN$  is expressed as follows, considering the volume element of integral:

$$\frac{\mu_0}{4\pi} |\vec{\mu}|^2 \frac{1}{r^3} = \frac{3}{2} k_B T_i dN = \frac{3}{2} k_B T_i \times g f d\vec{k}. \quad (\text{A-4-1})$$

$$d\vec{k} = \frac{1}{dv} = \frac{1}{\frac{4\pi}{3} r^3}. \quad (\text{A-4-2})$$

Thus, here, an important equation is derived.

$$\mu_0 |\vec{\mu}|^2 = \frac{9}{2} k_B T_i g f = \frac{9}{2} k_B T_i g \frac{1}{\exp\left(-\frac{E_i - E_F}{k_B T_i}\right) - 1}. \quad (\text{A-5})$$

In this Bose-statistic equation,  $E_i$  denotes the zero-point energy of phonon, i.e., the Debye temperature and  $+|E_F|$  is a chemical potential, which equals to Gibbs free energy, but especially this case implies only an internal energy. Therefore, this chemical potential is derived from electron specific heat coefficient as follows:

$$\mu_0 |\vec{\mu}|^2 = \frac{9}{2} k_B g \frac{T}{\exp\left[-\frac{1}{k_B T} \left(\frac{3}{2} k_B \theta_D + \gamma T^2\right)\right] - 1}, \quad (\text{A-6})$$

In this case, a transition temperature of  $T_c$  is assumed to be obtained by taking the extremum from this equation. Hence, to calculate differentials,  $T_i$  is considered to be a variable continuous temperature  $T$  because there are now no dependent parameters on index  $i$  except  $T_i$ .

Therefore, the following equation is calculated.

$$\frac{d}{dT} \mu_0 |\vec{\mu}|^2 = 0, \quad (\text{A-7})$$

Consequently, this equation is obtained:

$$\frac{\gamma T^2 - \frac{3}{2} k_B \theta_D}{k_B T} = -1, \quad (\text{A-8-1})$$

$$T \equiv T_c = -\frac{k_B}{2\gamma} + \sqrt{\frac{3k_B \theta_D}{2\gamma}} \approx \sqrt{\frac{3k_B \theta_D}{2\gamma}}, \quad (\text{A-8-2})$$

Table 1-A lists the physical constants of a ferromagnetic metal Fe.

Table 1-A Fe physical constants

Debye temperature $\theta_D$	470 K
Electron specific heat coefficient $\gamma$	$8.4 \times 10^{-27} \text{ J/K}^2$

Employing these physical constants, the transition temperature  $T_c$  for the metal Fe is calculated as

$$T_c \approx 1.08 \times 10^3 \text{ K} \quad (\text{A-9})$$

Because measurements of the transition report 1043 K, the agreement is sufficient.

Then, we consider the transition temperature of the ferromagnetic Ni. The material Ni has much less thermal conductivity, different from the metal Fe. This implies that a chemical energy, i.e, the internal thermal energy is allowed to be ignored. Thus, from eq. (A-8-1), the  $T_c$  equation is expressed simply as

$$\frac{3}{2} k_B \theta_D \approx k_B T_c. \quad (\text{A-10})$$

Because the Debye temperature of Ni is reported as 450 K, the  $T_c$  is calculated as

$$T_c \approx 675 \text{ K} \quad (\text{A-11})$$

Compared with a measured transition value 627 K, the agreement can be considered as sufficient.

## References

- [a1] P.W. Anderson, "Basic Notions of Condensed Matter Physics (The Benjamin Cummings, 1984)
- [a2] H.E. Stanley, "Introduction of Phase transitions and Critical phenomena (Oxford Univ Press, 1997)
- [a3]R. Shankar, *Rev. Mod. Phys.* **66**, 129 (1994)
- [a4] P.C. Hohenberg, *Phys. Rev.* **158**, 383 (1967)
- [a5]J.M. Kosterlitz and D.J. Thouless, *J. Phys. C*, **6**, 1181 (1973)
- [a6]J. Solyom, *Adv. Phys.* **28**, 201 (1979)